microplastics

MDPI

Article

Removal of Co-Occurring Microplastics and Metals in an Aqueous System by Pristine and Magnetised Larch Biochar

Stuart Cairns [1,*], Peter J. Holliman [2], Iain Robertson [1] and Benjamin Harrison [3]

[1] Department of Geography, Faculty of Science and Engineering, Swansea University, Swansea SA2 8PP, UK
[2] Materials Science and Engineering, Faculty of Science and Engineering, Swansea University, Swansea SA1 8EN, UK
[3] Chemical Engineering, Faculty of Science and Engineering, Swansea University, Swansea SA1 8EN, UK
* Correspondence: s.l.cairns@swansea.ac.uk

Abstract

Microplastics and metals are increasingly recognised as major water contaminants with profound environmental and health consequences. The environmental co-occurrence of microplastics and metals are well documented in waterways, including urban runoff, highway balancing ponds, industrial wastewater, and mine-impacted waters, posing a multifaceted environmental threat. Urgent remedial action is required to remove co-occurring microplastics and metals from water, giving consideration to how their co-occurrence can affect remediative efforts. However, information on the sorption of microplastics and Pb and Zn simultaneously by biochar is lacking. In this current study, changes in the quantity of metal adsorbed by pristine larch biochar and magnetised larch biochar due to the presence of microplastics was assessed using spectroscopic techniques. This study demonstrated that magnetised larch biochar and pristine larch biochar both remove co-occurring microplastics, Pb, and Zn from solution. Neither magnetised larch biochar nor pristine larch biochar show any statistical difference in the sorption of Pb with the inclusion of microplastics into the aqueous matrix. However, the inclusion of microplastics result in the reduced sorption of Zn by 43% for magnetised larch biochar ($p < 0.01$) and 69% for pristine larch biochar ($p < 0.01$). Magnetised larch biochar also demonstrated greater sorption than pristine larch biochar for microplastics ($p < 0.05$), Zn co-occurring with microplastics ($p < 0.05$), and Zn with no microplastics present ($p < 0.01$). Despite the effects of competitive sorption between Zn and microplastics, the removal of Pb, Zn, and microplastic from a multi-contaminant system indicate that magnetic larch biochar is a viable option to remove multiple contaminants from aqueous environs where metals and microplastics are seen to co-occur.

Keywords: microplastic; biochar; metals; competitive sorption; co-occurring contaminants; sorbent

Academic Editor: Nicolas Kalogerakis

Received: 13 June 2025
Revised: 1 August 2025
Accepted: 15 August 2025
Published: 26 August 2025

Citation: Cairns, S.; Holliman, P.J.; Robertson, I.; Harrison, B. Removal of Co-Occurring Microplastics and Metals in an Aqueous System by Pristine and Magnetised Larch Biochar. *Microplastics* **2025**, *4*, 54. https://doi.org/10.3390/microplastics4030054

1. Introduction

Microplastic presence in freshwater has become an emerging global issue, heightened by their co-occurrence with metals, with extensive environmental and health consequences. Since the start of commercial mass production in the 1950s, societal reliance on plastic has made it a ubiquitous presence globally, with the potential for this emerging contaminant to combine with the emerged heavy metal pollutant causing environmental and human health consequences [1,2]. Current estimates of plastic production are as high as

400 million tonnes per year, with around 60% of this being disposed of into the environment [3]. Whilst the versatility of plastics has been of great societal benefit, the "plastic age" comes with the issue of plastic accumulation in the aquatic environment, with over 23 million tonnes of plastic entering our waterways on an annual basis [4,5]. Microplastic contamination has several diffuse and point sources, including vehicle emissions, textile washing, domestic secondary plastics, municipal wastewater sludge used for agriculture, urban runoff, and wastewater discharges from wastewater treatment plants [6].

The introduction of microplastic into aquatic environs effects growth, development, reproduction, and neurological functions of aquatic species [7]. An estimated 39,000–52,000 plastic particles are ingested per person annually thorough the consumption of these aquatic species [8]. Whilst the full impact on human health due to the bioaccumulation of microplastics in the body is not yet comprehensively understood it is believed to comprise harmful effects on the nervous system, kidney system, respiratory system, digestive system, and placenta [6]. The presence of additives used in plastic production as well as pollutants sorbed to the microplastics environmentally, such as metals, polycyclic aromatic hydrocarbons (PAHs), and polychlorinated biphenyls (PCBs), can be ingested with the microplastics and have been recognized as having carcinogenic and mutagenic effects on humans [9].

The co-occurrence of microplastics and heavy metals in freshwater environs are of increasing concern. Microplastic pollutants have been observed to combine with heavy metals, affecting ecosystems and living organisms [2]. Anthropogenic activities, such as the exponential rise in motor vehicles, mining, and industrial processes are considered to be the primary contributors to the increase in heavy metal aqueous contamination [10–12]. Tyre wear and exhaust particles, Pb and Zn mines, and industrial processes, such as electroplating and metal finishing, result in the continuous introduction of Pb and Zn into the environment [13–15]. Mine tailing ponds have been seen to have Pb concentrations as high as 146 mg/L and Zn concentrations as high as 150 mg/L [13]. Elevated concentrations of Pb and Zn are toxic, leading to disruption of freshwater ecosystems and negative impacts on human health, including neurological impacts, reduced liver function, reduced fertility, kidney damage, lung damage, and mortality [16]. Microplastics are vectors for heavy metals, such as Pb and Zn, transporting metals from urban environments and industrial and mine sites to water resources [17]. Polymers, such as polystyrene and polyethylene, have a particular adsorption affinity to heavy metals [2]. The co-occurrence and interactions between heavy metals and microplastics are being increasingly studied. The co-occurrence of polystyrene with Pb and/or Zn has been observed in the Chao Phraya River (Thailand), Lake Garda (Italy), and Pearl River, with sources of contamination including industrial wastewater and urban runoff [18–20]. Khant et al. [2] highlighted the significant environmental risks associated with high metal concentrations, originating from mine tailings, combining with microplastics and their subsequent combined transport over large distances through waterways. As a result of co-occurrence, researchers are increasingly showing significant interest in the combined effect of microplastics and heavy metals on the environment. Combined exposure to heavy metals (including Pb) and polystyrene has been seen to enhance the negative effect of heavy metals with increased accumulation and particle retention in terrestrial and aquatic organisms with the consequence of enhancing toxicity [21]. The ingestion of microplastics and heavy metals by aquatic species also results in their subsequent transfer up the food chain, with resultant human health implications [22].

The co-occurrence of Pb, Zn, and polystyrene are not only important in terms of the transport, toxicity, and bioavailability, but consideration must also be given to how their presence together can affect remediative efforts [23,24]. Whilst it is acknowledged that strategies to remove microplastics, Pb, and Zn from waterways must be adopted due to

environmental and human health concerns, the combination of microplastics and metals in a multi-contaminant system can change the characteristics of these individual materials. This has the potential to affect the removal of the co-occurring metal and microplastics from water [25,26].

In this context, biochar is a material that should be considered in the remediation of a microplastic and metal multi-contaminant aqueous system. Biochar is a porous, carbonaceous material produced by pyrolysis at temperatures between 350–1000 °C under limited oxygen conditions [27]. Alongside the benefits of biochar, including carbon sequestration and soil fertility, it has been proven to remove contaminants from aqueous media [28]. Biochar has been studied in the sorption of (post)-transition metals from aquatic environments, such as mine wastewater, motorway runoff, and groundwater, with key removal mechanisms including ion exchange, co-precipitation, electrostatic attraction, and π-π interactions [29]. Whilst biochar is well established as a material to adsorb metals from waterways, its use to remove microplastics is in its infancy. To date, the use of biochar has primarily focused on the removal of microplastics from single-contaminant aqueous systems or systems containing a variety of microplastics polymers [6,30,31]. The incorporation of microplastics as part of the biochar feedstock to increase metal removal has also been an area that has been investigated, as has the removal of co-occurring Cd, Ni, Cu, and microplastics [32,33]. However, the removal of microplastics co-occurring with Pb and Zn, which are primary motor vehicle, industrial, and mining pollutants, has not been explored to date.

The objective of this study is, therefore, to understand if pristine larch biochar and/or magnetised larch biochar can be used to effectively remove co-occurring Pb, Zn, and microplastics from an aqueous solution by (i) quantifying Pb and Zn removal by larch biochar and magnetised larch biochar in the absence of microplastics, (ii) identifying biochar sorption mechanisms of Pb and Zn in the absence of microplastics, (iii) quantifying the removal of microplastics, Pb, and Zn by larch biochar and magnetised larch biochar in a multi-contaminant system, and (iv) identifying any changes in sorption as a result of the co-occurrence of MPs, Pb, and Zn.

2. Materials and Methods

European larch (*Larix decidua* Mill.) wood chips were pyrolyzed at scale in a Pyrocal BigChar-1000 pyrolysis–gasification kiln at a temperature of ~550 °C, with a retention time of ~100 s. Previous studies have demonstrated the efficacy of larch as a feedstock to remove Pb and Zn from aqueous solutions, including mine-impacted water, due to the presence of oxygenated functional groups [13,34]. Furthermore, in the limited number of studies that discuss the removal of microplastics from aqueous by biochar, woody feedstock has been seen to be effective, with characteristics including an irregular rough structure which aids in trapping microplastics [35], a large SSA with a higher proportion of meso- and macropores, enabling microplastics to enter the pore structure [36], and a honeycomb structure that traps the microplastics, causing them to lose their mobility [37]. Pristine larch biochar was magnetised to increase chemisorption rather than focus solely on physisorption. Magnetisation has been seen to increase Pb and Zn sorption as well as PS sorption in single-contaminant solutions through complexation as well as hydrophobic and electrostatic interactions [30,38–40]. Other biochar modifications that have been used to increase microplastic removal have focussed on increasing surface area rather than trying to incorporate chemisorption into removal mechanisms [36]. Pristine larch biochar was magnetised using iron (III) chloride hexahydrate ($FeCl_3.6H_2O$) and iron (II) sulphate heptahydrate ($FeSO_4.7H_2O$) suspension. Briefly, pristine larch biochar was mixed with deionised water (DI) at a ratio of 1 g–10 mL. Separately, iron (III) chloride hexahydrate

($FeCl_3.6H_2O$) and iron (II) sulphate heptahydrate ($FeSO_4.7H_2O$) were mixed with DI water at a ratio of 1 g–0.57 g–30 mL. These ratios align with Shang et al. [41] in their magnetisation of biochar. The $FeCl_3.6H_2O$ and $FeSO_4.7H_2O$ mixed suspension was added to the biochar suspension and the pH was adjusted to 10.5 with the dropwise addition of an NaOH solution (10 mol/L). This suspension was bubbled under an N_2 atmosphere for one hour whilst being stirred vigorously at 25 °C. It was then boiled for one hour at 80 °C before being cooling for two hours at room temperature. The biochar, $FeCl_3.6H_2O$, and $FeSO_4.7H_2O$ suspension was filtered and washed repeatedly with DI water and then with ethanol until a neutral supernatant was achieved. Finally, the resultant material was dried at 70 °C for 12 h. Pristine larch biochar and magnetised larch biochar are referred to as BC and MBC throughout the study, respectively.

2.1. Biochar Characterisation

Pristine larch biochar (BC) and magnetised larch biochar (MBC) were characterised via Fourier transform infrared spectroscopy (FTIR), scanning electron microscopy with energy dispersive X-ray (SEM-EDX) analysis, zeta potential analysis, elemental analysis (C, H, N, O, and S), specific surface area (SSA) analysis, X-ray powder diffraction (XRD), and total metal characterisation. FTIR analysis was undertaken using a Perkin Elmer Spectrum Two FTIR spectrometer (Beaconsfield, UK) with measurements in the range of 400–4000 cm^{-1} to compare possible changes before and after sorbent loading. Surface morphology and the presence of contaminants were examined by SEM-EDX analysis (Hitachi TM3000 desktop microscope, Slough, UK) using a working distance of 10 mm and an acceleration voltage of 15 kV; images were obtained using the internal Hitachi TM3000 software. The zeta potentials were measured for each biochar using a Zetasizer Nano ZS, Malvern Instruments (Santa Clara, CA, USA). All biochars were analysed for their CHNOS elemental composition using a Thermo FlashSmart CHNS/O elemental analyser (Loughborough, UK). Specific surface area was determined from N_2 physisorption isotherms using the Brunauer–Emmett–Teller method. Vacuum-dried samples were degassed overnight at a temperature of 105 °C and measured with N_2 adsorption at a liquid nitrogen temperature of −196 °C by a NOVA 2000e surface area and pore size analyser (Leighton, Buzzard, UK). XRD was used to identify magnetic characteristics. XRD patterns were obtained using a Bruker D8 Discover (Karlsruhe, Germany) with a copper source (40 kV, 40 mA) and a 1D detector. Powdered MBC was pushed flat on a single signal silicate zero diffraction plate to minimise background interference. The scans themselves had a 0.5 s time per step and an increment of 0.02° over the range of 10–90. The total metal concentrations of each biochar were determined by inductively coupled plasma–optical emission spectroscopy (ICP-OES) using an ICP-OES 5110, Agilent Technologies Inc., USA (Santa Clara, CA, USA). Prior to characterisation, samples were prepared using microwave-assisted digestion, where 20 mg of each sample of biochar was digested in the presence of 6 mL HNO_3, 2 mL HCl, and 0.5 mL HF and filtered through a 0.45 µm cellulose acetate filter post-digestion.

2.2. Sorption Experiments

2.2.1. Batch Sorption: Study Metal

Batch sorption experiments were carried out using $Pb^{2+}_{(aq)}$ and $Zn^{2+}_{(aq)}$ with concentrations of 20 mg/L, 50 mg/L, 100 mg/L, 150 mg/L, and 200 mg/L. This range was selected to reflect the extreme concentrations of Pb and Zn reported in industrially polluted waters, mine-impacted waters, and tailing ponds, with these concentrations ranging from 15 mg/L to 33 mg/L in industrial wastewater, 12.7 mg/L to 68.4 mg/L in mine-impacted water, and up to 150 mg/L in tailing ponds [13,42–45]. Analytical-grade chemical reagents obtained from Fischer Scientific (Loughborough, UK) were used to prepare a stock solution

(1000 mg/L) of $Pb(NO_3)_2$ and $Zn(NO_3)_2 \cdot 6H_2O$ by diluting them with DI water. The pH for each concentration was adjusted to ~6.0 with dropwise addition of HNO_3 and NaOH. This pH was selected to be representative of the neutral mine drainage, mine-impacted water, and tailing pond pH of between 5.6 and 6.4 [13,46].

BC and MBC were dried for 24 h at 105 °C, and 0.1 g of biochar was added to 20 mL of aqueous solution in 25 mL glass McCartney bottles [47]. Previous studies have demonstrated that equilibrium was achieved by 24 h; thus, samples were agitated on a Unitwist 400 Orbital Shaker (Martinsried, Germany) for 24 h at ~280 rpm to reach equilibrium [34]. The pH of each sample was measured using a calibrated Hanna Edge pH meter (Leighton Buzzard, UK) before allowing the samples to settle for 24 h. The supernatant was removed and filtered with a 0.45 µm PTFE syringe filter for elemental analysis. Two types of control experiments were included, namely biochar without contaminants and contaminants without biochar. All experiments were performed in triplicate using a batch sorption equilibrium method [48]. Pb and Zn concentrations of the acidified supernatants were measured using microwave plasma atomic emission spectroscopy (MP-AES 4200, Agilent, Stockport, UK). Sorbent loading (q) was calculated from the difference between the initial metal concentration and final metal concentrations in the aqueous phase, as follows:

$$q = \left(c_i - c_{aq}\right) V / W$$

where c_i is the initial concentration of metals in the solution, c_{aq} is the final equilibrium concentration of metals in the solution, V is the volume of the solution, and W is the weight of the biochar.

2.2.2. Batch Sorption Study: Microplastic and Metal

Sorption batch experiments were carried out using 2 µm carboxylate-modified fluorescent red polystyrene beads (Analytical grade, Merck Life Science, Gillingham, UK). Polystyrene was selected as it is one of the most fabricated polymers globally and has a high affinity for Pb and Zn [2,49]. It is also routinely found in water, co-occurring with Pb and Zn, and has a density lower than water, making it less liable to fall out of the water column environmentally [18,20,50]. Spheres were selected as an environmentally occurring shape that are harder to sorb than other environmentally found plastic shapes, such as fragments or fibres due to the smoothness of the surface [37]. Five different polystyrene solution concentrations were used, with concentrations of 5 mg/L, 10 mg/L, 20 mg/L, 30 mg/L, and 50 mg/L alongside Pb and Zn in the range of 20 mg/L to 200 mg/L. The concentration range of the polystyrene beads was selected to reflect the extreme microplastic concentrations measured in a number of environs. Concentrations of MPs in lakes have been reported as high as 4.6 mg/L; in industrial sites, concentrations are as high as 6.2 mg/L; in stormwater runoff, concentrations are as high as 13 mg/L; in rivers, concentrations are as high as 26 mg/L; and in balancing ponds, concentrations are as high as 29.8 mg/L [51–54]. These concentrations were selected to stress the biochars to the maximum that would be encountered in field conditions. The five concentrations of polystyrene beads were obtained by preparing a stock solution (100 mg/L) and diluting it with the Pb and Zn stock solution and DI water. The pH for each concentration was again adjusted to ~6.0 with the dropwise addition of HNO_3 and NaOH. Solutions were prepared using glass flasks and bottles to minimise the loss of MPs as a result of electrostatic bonds to container walls. MP solutions were sonicated and vigorously stirred before application at each stage to guarantee homogeneity.

The BC and MBC were dried for 24 h at 105 °C and 0.1 g of biochar was added to 20 mL of aqueous solution in 25 mL glass McCartney bottles. Agitation was achieved on a Unitwist 400 Orbital Shaker for 24 h at ~280 rpm to reach equilibrium. The pH of each sample was

then measured using a calibrated Hanna Edge pH meter before allowing the samples to settle for 24 h and before removing the supernatant. Two 5 mL aliquots of supernatant were removed from each sample, one for metal analysis and one for microplastic (MP) analysis.

To measure the remaining concentration of Pb and Zn in solution, each sample was analysed using MP-AES, as with the metal-only solution. The supernatant used for MP analysis was removed and filtered with a 3 µm PTFE syringe filter for analysis. To measure the remaining concentration of MPs in solution, each sample was analysed using fluorescence spectroscopy (Perkin Elmer LS 55 Fluorescence Spectrophotometer, Stockport, UK) with 575 nm excitation and 550–640 nm emission wavelengths. The calibration curve is shown in Supplementary File S1.

2.3. Water Chemistry and Metal Speciation

Speciation analysis of the Pb and Zn solution followed by the Pb, Zn, and MP solution was carried out using the PHREEQC code (version 3.7.1) and the MINTEQV4 database [55]. The pH, temperature, and concentrations of base cations, metal contaminants, alkalinity and nutrients were used as model inputs. Samples contaminated at 20 mg/L Pb and Zn and 20 mg/L Pb and Zn with 5 mg/L MP were analysed to determine mobile and immobile speciation of the Pb and Zn.

Samples with and without contaminants at a selected concentration of 20 mg/L Pb and Zn and 20 mg/L Pb and Zn with 5 mg/L MP were analysed for other water chemistry parameters. These included (i) base cation analysis (Ca and Mg) using MP-AES, (ii) major anions (Cl^-) using an ion exchange chromatograph (IC 930 Compact Flex, Metrohm, Herisau, Switzerland), and (iii) P and Si via ICP-OES (Agilent ICP-OES 5110 Santa Clara, CA, USA).

2.4. Statistical Analysis

Comparisons between MBC and BC contaminant removal values were performed using the Mann–Whitney U test [56].

3. Results and Discussion

3.1. Contaminant Removal by Pristine Larch Biochar and Magnetised Larch Biochar

Magnetised larch biochar (MBC) and pristine larch biochar (BC) both removed Pb and Zn in a multi-metal solution and microplastics (MPs), Pb, and Zn in a combined MP and metal solution. MBC increased metal removal in a multi-metal solution as compared to BC with significantly greater Zn removal ($p < 0.05$) (Figure 1A). MBC also showed greater removal of polystyrene microplastics (MPs) from solution than pristine larch biochar (BC), particularly at higher initial MP concentrations ($p < 0.05$) (Figure 1B). The addition of MP to the aqueous matrix resulted in a decrease in the MBC removal of Zn by 43% and the BC removal of Zn by 69% suggesting competition for sorption sites between MPs and Zn. Although this decrease was evident for both biochar treatments, the decrease was significantly less for MBC than BC ($p < 0.01$). The removal of Pb by MBC and BC remained broadly level once MP was added to solution (Figure 1A). The maximum measured removal of Pb in the metal-only solution by MBC was 16.19 mg/g (±0.18), while it was 17.51 mg/g (±0.46) in the combined MP and metal solution; the maximum measured removal of Zn in the metal-only solution by MBC was 10.89 mg/g (±0.72), while it was 6.26 mg/g (±0.07) in the combined MP and metal solution; the maximum measured removal of MP by MBC was 34.10 mg/L (±3.11). The maximum measured removal of Pb in the metal-only solution by BC was 14.07 mg/g (±0.18), while it was 13.82 mg/g (±1.53) in combined MP and metal solution; the maximum measured removal of Zn in the metal-only solution by BC was

9.89 mg/g (±0.31), while it was 3.03 (±0.88) in the combined MP and metal solution; the maximum measured removal of MP by BC was 22.58 mg/L (±4.64).

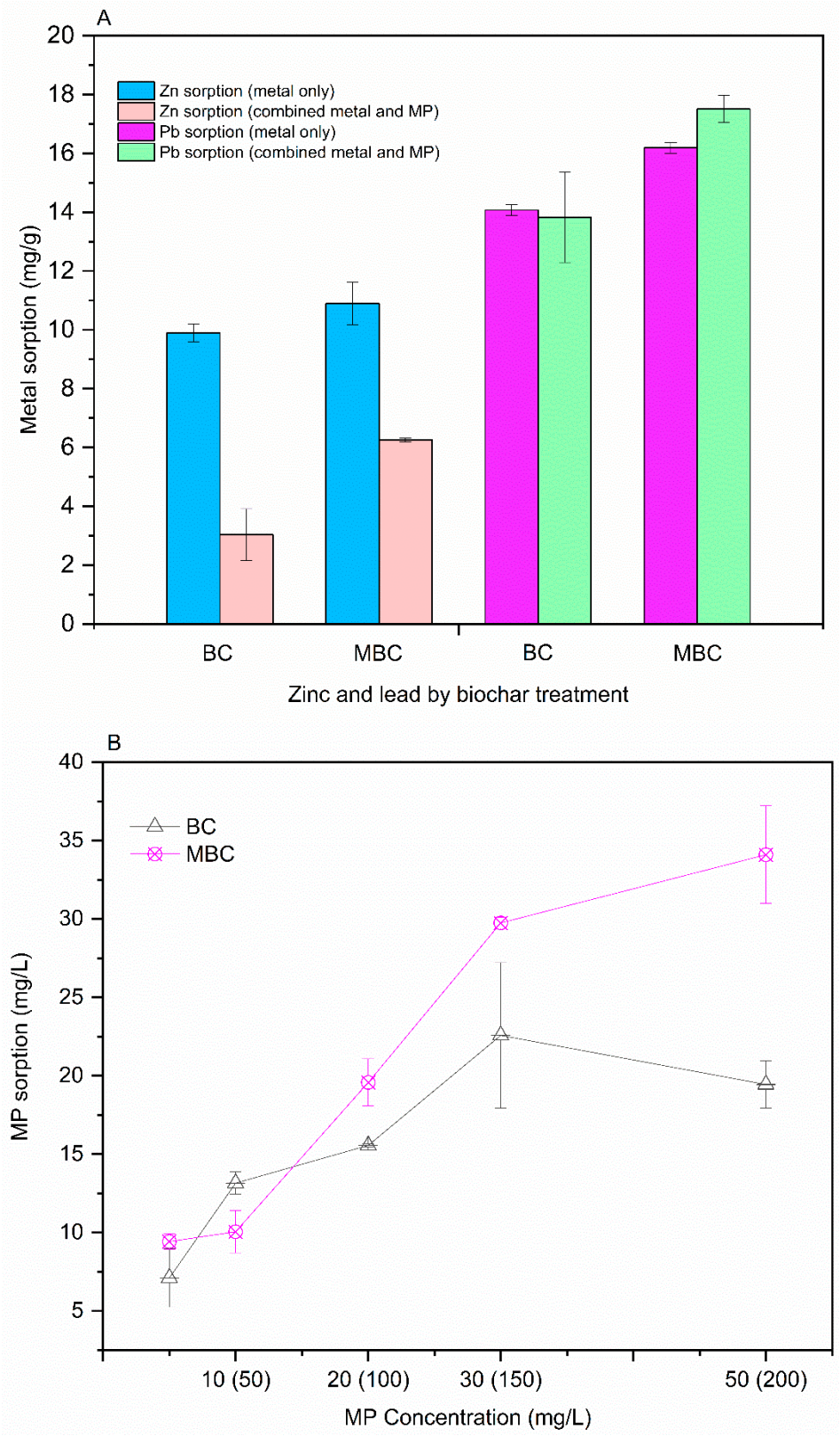

Figure 1. (**A**) The removal of Pb and Zn by pristine larch biochar (BC) and magnetised larch biochar (MBC) in a metal solution and a metal and polystyrene microplastic (MP) solution. (**B**) The removal of polystyrene microplastic (MP) by BC and MBC in the presence of Pb and Zn.

Whilst these removal values indicate competitive sorption between MP and Zn, it was found that the adsorption of MP does not outcompete Pb. The difference between the interaction of the two metals with MP is a reflection of how Pb and Zn interact with each other. Competitive sorption between Pb and Zn is well documented, with Pb regularly outcompeting Zn in sorption studies [16,34,57]. Pb has a larger ionic radius (0.118 nm) than Zn (0.074 nm) leading to the larger Pb ions preferentially displacing the smaller Zn ions [58]. In addition, Pb has a greater affinity than Zn with functional groups due to its higher electronegativity and lower pK_H [59,60].

3.2. Biochar Characterisation

The physicochemical properties of both BC and MBC have been investigated to better understand the relevance of the materials' characteristics in relation to MP, Pb, and Zn sorption (Table 1). XRD analysis demonstrated that MBC had peaks at 30.43, 35.73, 43.35, 53.73, 57.43, and 63.03, which corresponded to the (220), (311), (400), (422), (511), and (440) lattice plains of Fe_3O_4, respectively, confirming that MBC was successfully loaded with Fe_3O_4, ensuring the attendant magnetic characteristics (Figure 2) [30]. This was further supported by the attraction of MBC to external magnetic forces (Supplementary File S2). The elevated O/C ratio determined by elemental analysis indicates that MBC has a greater proportion of surface functional groups than BC (Table 1). These are key to contaminant sorption. The elevated O/C ratio is a common phenomenon in the magnetising of biochar and is caused by iron oxide loading onto the material [61]. The O/C ratio, which is commonly accepted as an index for polarity and is intrinsically linked to the abundance of oxygenated functional groups [29], is more than two times higher for MBC than BC. The (O + N)/C ratio, also used as a proxy for polarity, was almost identical to the O/C as the content of N was extremely low. Inherently linked to this, the high O/C ratio also affects the hydrophobicity of the material leading to more hydrophilic surface characteristics which enable MPs to access sorption sites and, therefore, contribute to MP sorption [38]. The increase in O/C ratio for magnetised biochar has been, in part, attributed to the addition of metal oxides to the material intrinsic to the sorption process for MPs and metals [38,62]. The presence of Fe was confirmed by the ICP-OES characterisation of MBC (Table 1). Although a higher O/C ratio is associated with a negative charge and can cause electrostatic repulsion of anions, such as those seen on the surface of the carboxylate-modified MP, the biochar negative charge can be lessened or even overcome with magnetisation and the inherent deposition of positively charged Fe ions onto the surface of the magnetised biochar [29,39]. However, it should be noted that, conversely, this negative charge can increase sorption of positively charged metals, such as Pb^{2+} and Zn^{2+}, through electrostatic interactions [29]. The presence of these oxygenated functional groups is of relevance to metal sorption through ion exchange and complexation [13,63] and has also been seen to play a pivotal role in the removal of MPs through H-bonding interactions [64]. The H/C ratio of MBC was ~7% greater than that of BC, which indicates that the aromatic structure of BC was greater than MBC; this observation has been previously attributed to the addition of metal oxides, which can induce more rapid degeneration of the carbon phase [65].

Table 1. The physicochemical properties of pristine larch biochar (BC) and magnetised larch biochar (MBC).

Biochar Type	O/C	(O + N)/C	H/C	BET Surface Area (m^2/g)	Zn (mg/g)	Ca (mg/g)	Mg (mg/g)	P (mg/g)	Fe (mg/g)
BC	0.142	0.143	0.027	361.7	0.12	2.15	0.28	0.19	23.55
MBC	0.352	0.354	0.029	272.6	0.08	0.97	0.14	0.12	207.10

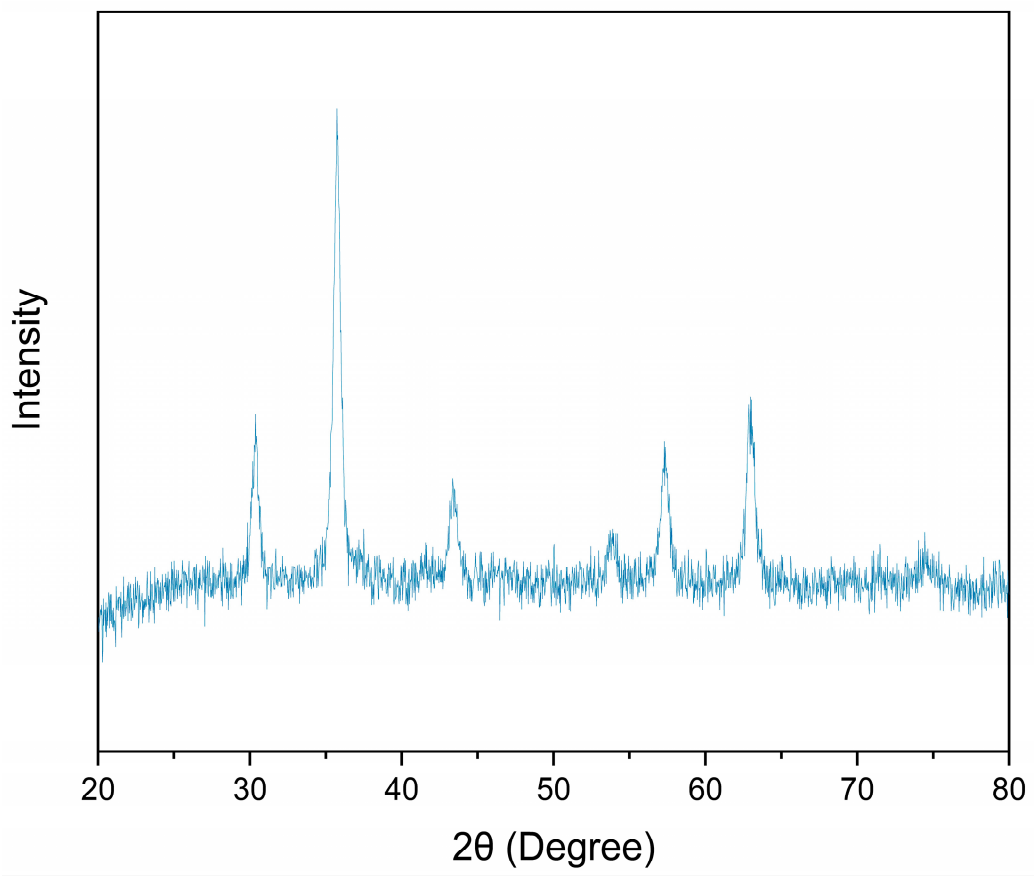

Figure 2. The XRD pattern of magnetised larch biochar (MBC).

The specific surface area (SSA) of MBC was lower than that of BC by 25%. Previous studies have highlighted the importance of the SSA for unmagnetized biochar in the sorption of MP and separately in the sorption of metals including Pb [31,66]. However, SSA is not always an indicator of contaminant removal, particularly if chemisorption rather than physisorption is the driving factor [29]. Even though BC was seen to have a higher SSA, MBC exhibited higher maximum measured removal of MP, Pb, and Zn which indicates that SSA was not the primary factor in the removal of these contaminants and that chemisorption was of relevance for MBC.

3.3. Materials Analysis

Analysis of MBC and BC was undertaken prior to sorption, post-metal sorption, and finally post-metal and MP combined sorption to investigate the mechanisms of contaminant removal from solution.

Fluorescence spectroscopy demonstrated the removal of MPs from solution (Figure 1B), and subsequent FTIR analysis evidenced the presence of these MPs on the surface of both MBC and BC. A new peak at the wavelength of 2981 cm^{-1} developed for both MBC and BC post-sorption of MPs (Figure 3A,B and Supplementary File S3a,b). This peak is associated with carboxyl functional groups [67] and is attributed to the carboxylate modification on the surface of the MPs. The appearance of the peak denotes the presence of the MPs on the surface of both chars.

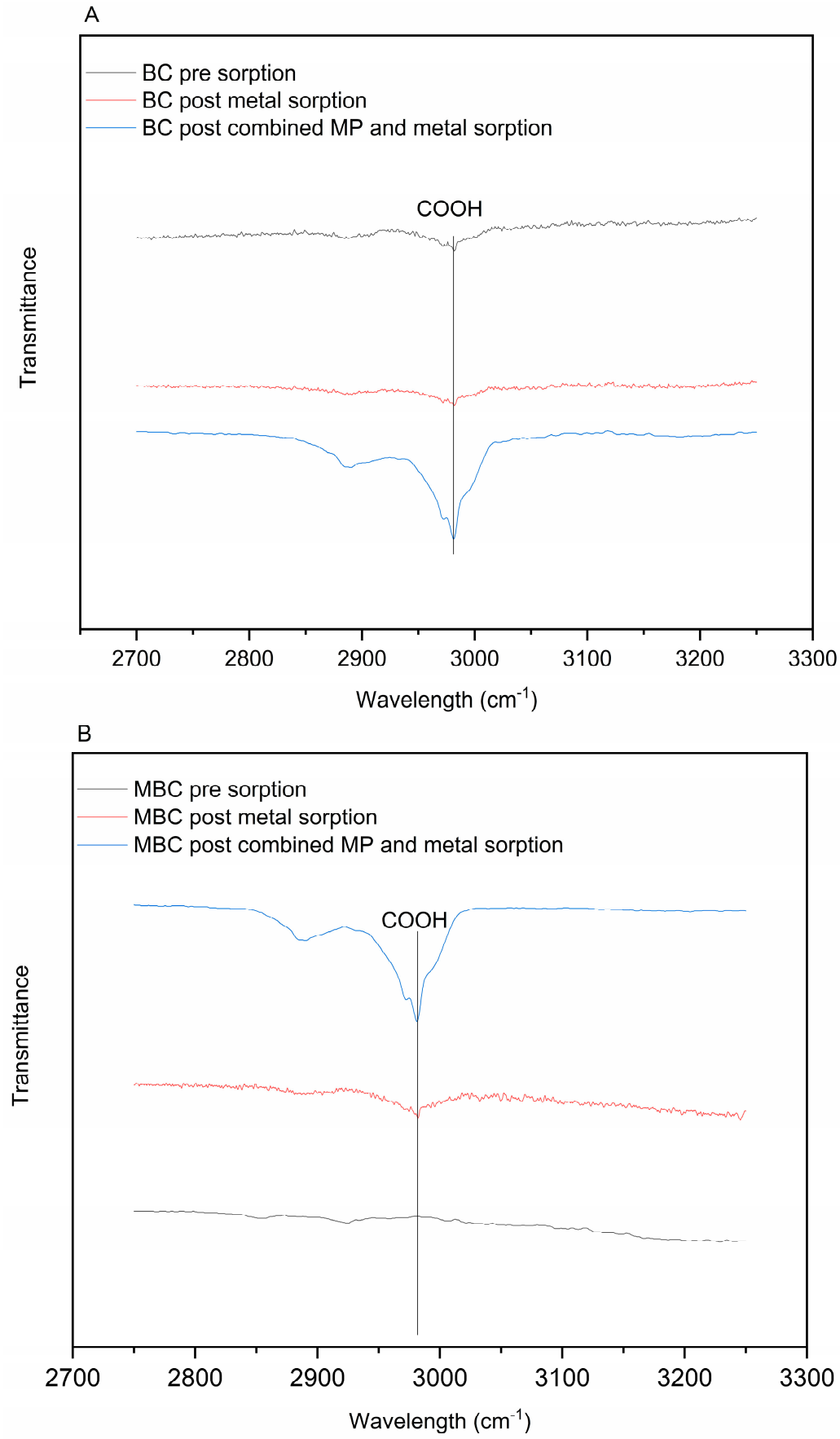

Figure 3. FTIR spectra for (**A**) pristine larch biochar and (**B**) magnetised larch biochar pre-sorption, post-metal-only sorption, and post-combined microplastic and metal sorption.

The presence of MPs was observed on the surface of both MBC and BC via SEM imaging (Figure 4A,C,D). The SEM imaging of BC demonstrates a morphology that resembles the honeycomb microstructure described by Wang et al. [37] (Figure 4B). This honeycomb structure is most commonly associated with biochar pyrolysed using a woody biomass feedstock [68], such as the larch used in this study. Wang et al. [68] proposed three main categories of MP retention intrinsically linked to the morphology and physisorption of the biochar, i.e., "stuck", "trapped", and "entangled". Stuck denoted the retention of MPs between the gaps in the material particles, with poor retention. Being trapped denoted MPs losing their mobility as they entered pores in the structure of biochar associated with honeycomb structures. Being entangled denoted microplastics being held in place by small biochar particles or "chips" which wrap around the microplastics, as seen where flaky shaped particles which are detached from the main structure of the material, "entangling" and immobilising the MP. The observed morphology of BC appears to lend itself to MPs becoming "trapped" in the pores due to the honeycomb structure of BC, and "entangled" due to the flaky BC particles wrapping around the MPs (Figure 4A). This indicates that physisorption is an important factor in the removal of MPs by BC and, as such, SSA is an important characteristic in MP removal for this biochar. However, SEM images demonstrate the presence of MPs amongst the iron oxide particles on the surface of the MBC, pointing to the importance of chemisorption as well as physisorption in the removal of MP by MBC (Figure 4C,D). The honeycomb structure of MBC can be seen pre-sorption (Figure 4E), but the large number of iron oxide particles appear to be blocking some pores leading to the lower SSA values than BC. The attachment of the iron oxides also resulted in an increased roughness of the surface of MBC, which has been seen to be a key feature in the trapping of MPs [39]. The spectral mapping of MBC demonstrates the presence of O alongside Fe in the absence of S and Cl (Figure 4D), which were both used in the magnetisation of MBC, indicating iron oxide-derivatised biochar [39]. The presence of these iron oxides is, in part, responsible for the presence of oxygenated functional groups potentially important in ion exchange, complexation, and a reduction in negative surface charge [69].

To explore the surface groups related to these contaminant removal mechanisms FTIR and SEM-EDX analysis was performed. The FTIR spectra for MBC showed abundant surface functional group peaks key to ion exchange and complexation (Figure 5A), and SEM-EDX mapping demonstrated the associated presence of the base cations Ca and Mg on the surface of MBC pre-sorption (Figure 4B and Supplementary File S4a,b). The FTIR spectra peaks at wavelengths of 1558, 1160, and 878/818 cm^{-1} relate to carbonyl groups, carboxyl groups, and aromatic C-H, respectively [30,67,70–72]. Once subjected to the metal-only solution, the peaks associated with the carbonyl and carboxyl group flatten slightly, and, in the case of the carboxyl group, shift, signifying that ion exchange is a key mechanism in the sorption of Pb and Zn by MBC (Figure 4D). However, these peaks flattened substantially more once MBC was subjected to the combined metal and MP solution. Surface functional groups play an essential role in the adsorption of MPs due to H-bond formation, and the disappearance of these peaks is a sign of the involvement of surface complexation in the MP sorption process [30,31]. The partial flattening of peaks post-metal sorption and the further flattening post-metal and MP sorption demonstrates that the sorption mechanism for metals and MP both rely on oxygenated functional groups, with Zn and MP most obviously competing for sorption sites. The reduced Zn sorption once MBC was subjected to the combined metal and MP solution strongly suggests that MPs are outcompeting Zn for these sites; conversely the absence of a reduction in Pb sorption in the presence of MPs indicates that MPs are not outcompeting Pb. The C-H peaks diminished once MBC were subjected to the combined metal and MP solution and are further evidence of H-bonding between MBC and MPs (Figure 5A). This peak does

not noticeably decrease post-metal sorption, indicating that H-bonding at these sites is not a relevant metal sorption mechanism and, therefore, is not relevant to any competitive sorption observed in this study. The C-H peak flattening is not evident in the BC FTIR spectra; MBC H-bonding with MPs is more prevalent than BC, at least partly explaining the higher sorption of MPs by MBC.

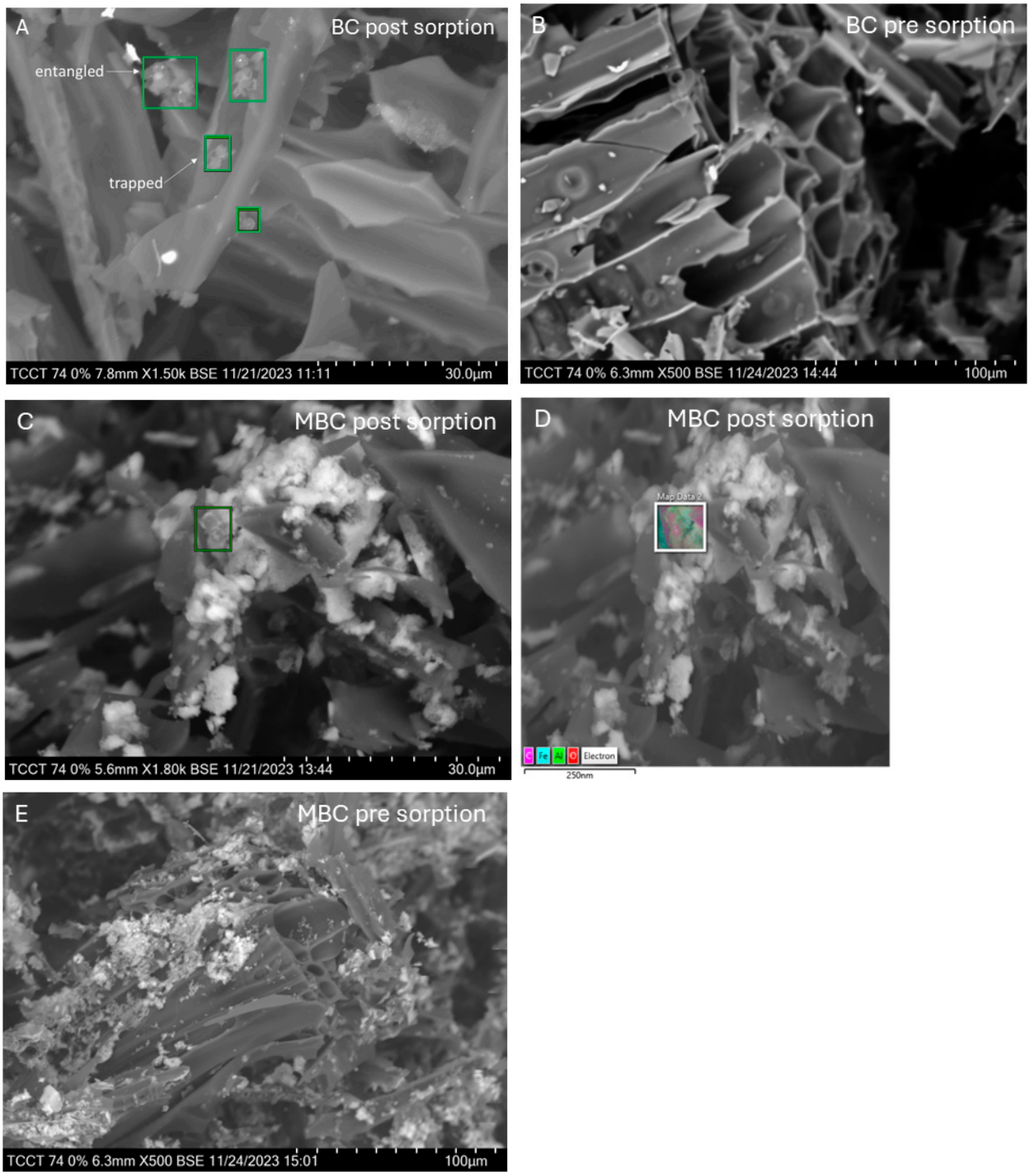

Figure 4. (**A**) SEM image of microplastics (MPs) which have been trapped and entangled by pristine larch biochar (BC), (**B**) SEM image of the honeycomb structure of BC, (**C**) SEM image of MPs amongst the Fe on the surface of magnetised larch biochar (MBC), (**D**) the EDX spectral mapping of the MPs on the surface of MBC, and (**E**) SEM image of the honeycomb structure of MBC with pores blocked by Fe.

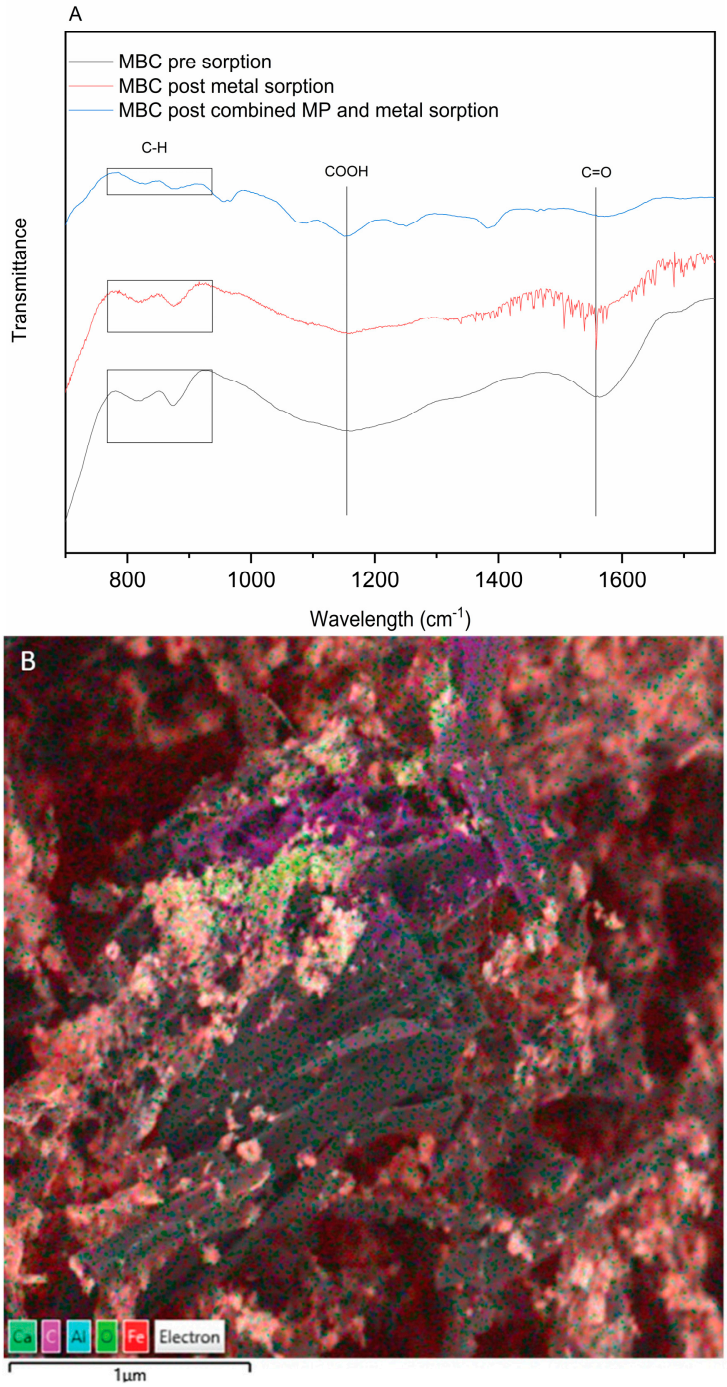

Figure 5. (**A**) FTIR spectra of MBC pre-sorption, post-metal sorption, and post-combined microplastic and metal sorption; (**B**) SEM image and EDX spectral mapping of iron oxide on the MBC surface.

3.4. Aqueous Phase Analysis

Aqueous phase analysis was undertaken to further understand the importance of ion exchange as well as investigate the potential role of co-precipitation, precipitation, and electrostatic interactions in contaminant sorption.

The importance of ion exchange in the sorption of Pb and Zn described by FTIR and SEM-EDX analysis, particularly for MBC, was confirmed by ICP-OES analysis. The increase in the release of cations, specifically Ca^{2+} and Mg^{2+}, are an indicator of ion exchange on the surface of the sorbent, where they are replaced by heavier metals, such as Pb^{2+} [73]. There is an obvious release of Ca and Mg by BC in the presence of contaminants but the proportional increase in the release of Ca and Mg is markedly greater for MBC, partly

explaining the increased sorption of Pb and Zn (Figure 6). Whilst cation release increases moderately from the metal solution to metal and MP solution, these increases can broadly be explained as being within experimental error (±1σ). With Pb sorption by MBC and BC showing no statistical change from the metal solution to the combined metal and MP solution and the marked decrease in Zn sorption, it should be assumed that ion exchange is a more important sorption mechanism for Pb than for Zn.

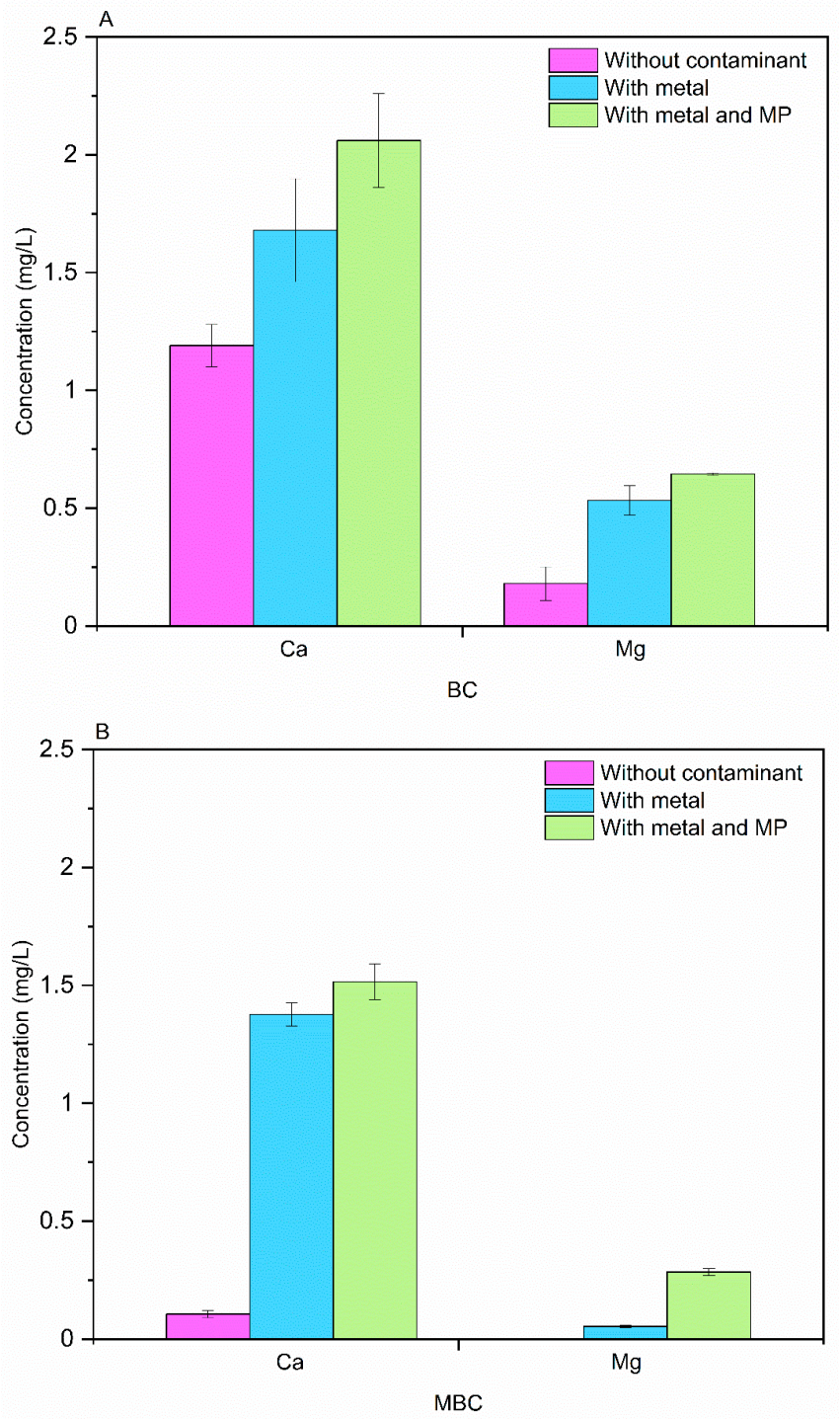

Figure 6. The changes in Ca and Mg concentrations in aqueous solution for (**A**) pristine larch biochar (BC) and (**B**) magnetised larch biochar (MBC).

Co-precipitation was seen to be a metal removal mechanism for BC. Phosphorus minerals have been seen to contribute to the sorption of Pb and Zn through precipitation

as insoluble phosphate salts [74]. The importance of phosphate-based ligands forming metal phosphate precipitates has been highlighted by Uchimiya et al. [73]. Differences in P (used as a proxy for PO_4^{3-}) and Si in the eluate of BC subjected to (i) a solution without contaminants, (ii) a solution with metal, and (iii) a solution with combined metal and MPs were examined to provide evidence for co-precipitation (Supplementary File S5). The higher the amount of P lost from the study materials to the eluate, the lower the amount of P that was available within MBC and BC to co-precipitate with metals [16]. The concentration of P in the BC eluate was at a maximum when subjected to solution without contaminants and was measured at 0.6 mg/L; this reduced to 0.17 mg/L when spiked with the combined metal and MP solution and reduced further to below the limit of detection when spiked with the metal solution. This indicates that some of the metal ions in solution are co-precipitating with the PO_4^{3-} when subjected to the metal solution but less so when subjected to the combined metal and MP solution. MPs appear to be limiting BC co-precipitation with metal. Due to the addition of Fe to the MBC, the proportion of P reduced and, as a result, the concentration of P in each of the MBC eluate samples was below the limit of detection.

The addition of anions, such as PO_4^{3-} and Cl^-, into solution can also play a part in the formation of metal precipitates, a phenomenon to which Zn is particularly susceptible to when conditions are favourable [34]. Speciation modelled by PHREEQC demonstrate that the proportion of immobile Zn is seen to decrease for both BC and MBC in the presence of MP with a distribution shift from hydroxyl and carbonate forms, such as $ZnCO_3$ and $ZnHCO_3$, to divalent forms of Zn. The reduction in immobile species as a result of the addition of MP is likely to reduce Zn removal from solution.

The potential for electrostatic repulsion between the negatively charged carboxylate MPs and MBC or BC was examined through the measurement of zeta potential. Biochar generally has a negative zeta potential at a pH of >5 unless surface modifications, such as magnetisation, are undertaken [6]. The zeta potential for MBC was significantly less negative than BC ($p < 0.05$). The less negative surface charge of MBC is primarily due to the Fe loading on the surface as demonstrated by SEM-EDX (Figure 4C–E) and ICP-OES characterization (Table 1), with the deposition of positively charged Fe ions causing this reduction in negativity. MBC displayed a negative zeta potential of −7.1 mV at the study pH of 6, as opposed to BC which had a more negative zeta potential of −22.4 mV; the zeta potential values of both MBC and BC showed a decreasing trend with increasing solution pH. The negative charge of the sorbent has the potential to electrostatically repulse the negatively charged MP. The strength of a repulsive zeta potential creates an energy barrier, and the interaction between the biochar and the MPs must exceed the primary energy barrier for sorption to take place [31]. The significant difference in zeta potential between MBC and BC leads to the repulsion potential barrier between MPs and MBC being significantly lower than the repulsion barrier between MP and BC enabling greater MP sorption by MBC [65]. Ganie et al. [75] further demonstrated that, in the range of −10 mV to +20 mV, the self-aggregation ability of MBC can cause self-precipitation of the reaction precipitate after MP interaction, further increasing MP sorption. Whilst this study was conducted at a pH of 6 to be representative of mine-impacted water and tailing pond pH of between 5.6 and 6.4, the zeta potential of MBC remains within the self-aggregation range outlined by Ganie et al. [75], up to and likely beyond pH 8 (Figure 7). The likelihood of increased removal of MPs at lower pH is in contrast to is the likely increase in Pb and Zn removal at higher pH where precipitation is probable and metals are less bioavailable. The reduced negative zeta potential, due to the addition of iron oxides to the surface of MBC, has the potential to overcome the MP metal tension in terms of water pH.

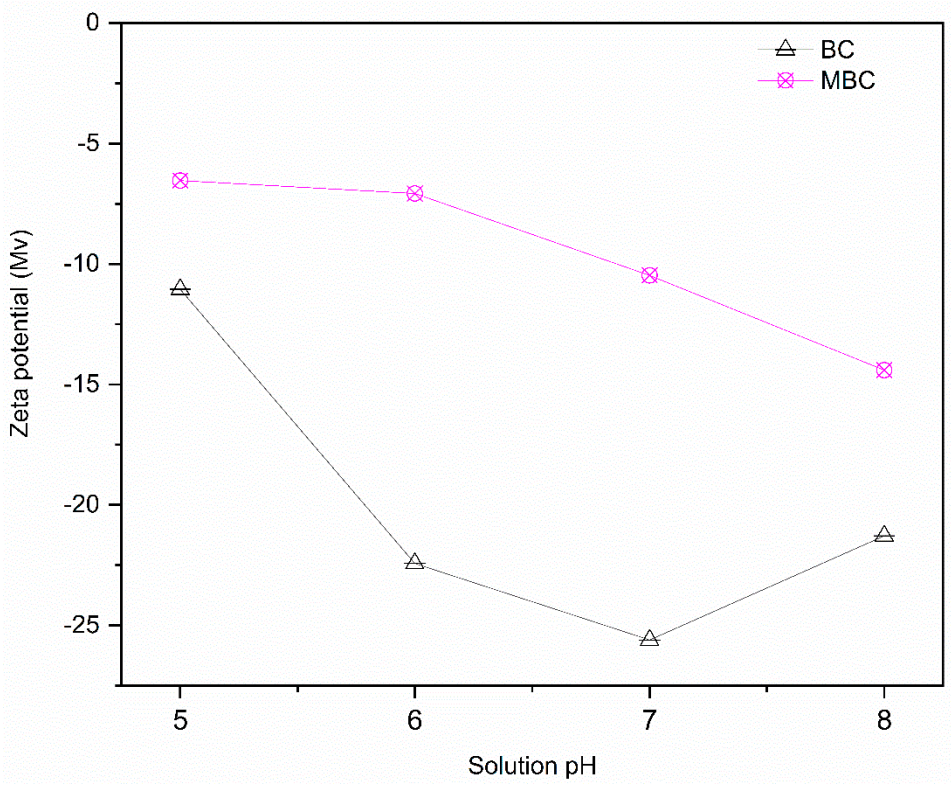

Figure 7. Zeta potential (mV) for pristine larch biochar (BC) and magnetised larch biochar (MBC).

The increase in divalent Ca and Mg cations in the effluent of both BC and MBC as a result of ion exchange with Pb and Zn (Figure 6A,B) has also been shown to have the attendant effect of increasing the ionic strength of the MP suspension [39]. This, in turn, has the effect of decreasing the MP negative charge, thus inhibiting the repulsive forces between the MP and the sorbent [65]. The multivalent cations released by MBC and BC, including Ca and Mg, also induce MP colloidal aggregation in addition to inhibiting electrostatic repulsion, with the resultant MP aggregates more readily retained in the carbonaceous sorbent pore structure [65].

4. Conclusions

Microplastics and metals are recognised as ubiquitous contaminants of concern with striking ecosystem and health consequences. The combined exposure to microplastic and heavy metals has been seen to enhance contaminant toxicity through increased particle accumulation and retention in terrestrial and aquatic organisms. As a result, the co-occurrence of microplastics and heavy metals in freshwater environs has received increasing attention. Despite this concern, information on the simultaneous removal of metals, such as Pb and Zn, and microplastics from water, in particular using biochar, is lacking. To date the use of biochar as a microplastic sorbent has primarily focused on the removal of microplastics from single-contaminant aqueous systems or systems containing a variety of microplastics polymers. The use of biochar to remove Pb and Zn, which are the primary metal pollutants associated with mine-impacted water, mine tailing ponds, and urban runoff, whilst co-occurring with microplastic, has not been reported previously. This study demonstrated that magnetised larch biochar (MBC) and pristine larch biochar (BC) both remove co-occurring MPs, Pb, and Zn from solutions with metal concentrations representative of industrially polluted water, mine-impacted water, and tailing ponds. Magnetising the biochar significantly increases the sorption of MPs and Zn. Increased removal of MPs was found to be due to a lessened electrostatic repulsion between the

surface of MBC and MPs, a result of the deposition of Fe cations onto the surface of MBC. MP removal was due to physisorption and chemisorption, with MBC physisorption enhanced by increased surface roughness and chemisorption driven by complexation. Ca and Mg cations released during ion exchange with heavier metals were also likely to have lessened the negative charge of MPs, reducing electrostatic repulsion with the sorbents and increasing MP removal. Zn removal by both MBC and BC reduced when metals co-occurred with MPs due to competition for and blocking of sorption sites and a reduction in Zn precipitation; this reduction was significantly higher for BC than MBC. Pb removal was not seen to reduce in the presence of MP as MP was not out competing Pb for sorption sites. Whilst MPs inhibit the removal of Zn by the studied sorbents, removal is still evident in conjunction with MP and Pb sorption. This study demonstrated both MBC and BC are viable options to remediate waters where MPs, Pb, and Zn co-occur, even where extreme contamination is found, such as industrially polluted water, mine-impacted water, and tailing ponds. The future direction of the study of biochar as a sorbent in waterways where MPs and metal co-occur needs to focus more heavily on the environmental parameters and environmentally sourced MPs that influence the efficacy of biochar, adopting a blended approach between laboratory and field studies to support technology diffusion. Methods to regenerate and reuse biochar that has reached sorption capacity should also be studied alongside the potential to valorise recovered MPs.

Supplementary Materials: The following supporting information can be downloaded at: https://www.mdpi.com/article/10.3390/microplastics4030054/s1, S1: The calibration curve for the 2 μm carboxylate modified fluorescent red polystyrene beads; S2: Image of the magnetic attraction of magnetised larch biochar (MBC); S3: Full FTIR spectra for (a) pristine larch biochar (BC) and (b) magnetised larch biochar (MBC) pre sorption, post metal only sorption and post combined microplastic and metal sorption; S4: (a) EDX analysis demonstrating the presence of Ca and Mg on the surface of magnetised larch biochar (MBC) pre-sorption (b) EDX weight and atomic percentages of Ca and Mg present on the surface of MBC; S5: Concentrations of P, Si and Cl^- without contaminants, with metal, and with metal and MP for pristine larch biochar (BC) and magnetised larch biochar (MBC).

Author Contributions: S.C.: Conceptualization, Formal analysis, Funding acquisition, Methodology, Investigation, Writing—Original Draft. P.J.H.: Writing—Review and Editing. I.R.: Writing—Review and Editing. B.H.: Methodology. All authors have read and agreed to the published version of the manuscript.

Funding: This research was funded by the Engineering and Physical Sciences Research Council (EPSRC), grant number EP/X525637/1.

Data Availability Statement: The original contributions presented in this study are included in the article/Supplementary Material. Further inquiries can be directed to the corresponding author.

Conflicts of Interest: The authors declare no conflicts of interest.

Abbreviations

The following abbreviations are used in this manuscript:

MP	Microplastics
BC	Pristine larch biochar
MBC	Magnetised larch biochar

References

1. Hale, R.C.; Seeley, M.E.; La Guardia, M.J.; Mai, L.; Zeng, E.Y. *A Global Perspective on Microplastics*; Blackwell Publishing Ltd.: Hoboken, NJ, USA, 2020. [CrossRef]
2. Khant, N.A.; Chia, R.W.; Moon, J.; Lee, J.Y.; Kim, H. Review on the relationship between microplastics and heavy metals in freshwater near mining areas. *Environ. Sci. Pollut. Res.* **2024**, *31*, 66009–66028. [CrossRef]

3. Chow, J.; Perez-Garcia, P.; Dierkes, R.; Streit, W.R. Microbial enzymes will offer limited solutions to the global plastic pollution crisis. *Microb. Biotechnol.* **2023**, *16*, 195–217. [CrossRef]
4. Wagner, M.; Scherer, C.; Alvarez-Muñoz, D.; Brennholt, N.; Bourrain, X.; Buchinger, S.; Fries, E.; Grosbois, C.; Klasmeier, J.; Marti, T.; et al. Microplastics in freshwater ecosystems: What we know and what we need to know. *Environ. Sci. Eur.* **2014**, *26*, 12. [CrossRef]
5. Borrelle, S.B.; Ringma, J.; Law, K.L.; Monnahan, C.C.; Lebreton, L.; McGivern, A.; Murphy, E.; Jambeck, J.; Leonard, G.H.; Hilleary, M.A.; et al. Predicted growth in plastic waste exceeds efforts to mitigate plastic pollution. *Science* **2020**, *369*, 1515–1518. [CrossRef] [PubMed]
6. Cairns, S.; Meza-Rojas, D.; Holliman, P.J.; Robertson, I. Interactions Between Biochar and Nano(Micro)Plastics in the Remediation of Aqueous Media. *Int. J. Environ. Res.* **2024**, *18*, 87. [CrossRef]
7. Toussaint, B.; Raffael, B.; Angers-Loustau, A.; Gilliland, D.; Kestens, V.; Petrillo, M.; Rio-Echevarria, I.M.; Van den Eede, G. Review of micro- and nanoplastic contamination in the food chain. *Food Addit. Contam. Part A* **2019**, *36*, 639–673. [CrossRef]
8. Cox, K.D.; Covernton, G.A.; Davies, H.L.; Dower, J.F.; Juanes, F.; Dudas, S.E. Human Consumption of Microplastics. *Environ. Sci. Technol.* **2019**, *53*, 7068–7074. [CrossRef] [PubMed]
9. Cverenkárová, K.; Valachovičová, M.; Mackul'ak, T.; Žemlička, L.; Bírošová, L. Microplastics in the food chain. *Life* **2021**, *11*, 1349. [CrossRef]
10. Beane, S.J.; Comber, S.D.W.; Rieuwerts, J.; Long, P. Abandoned metal mines and their impact on receiving waters: A case study from Southwest England. *Chemosphere* **2016**, *153*, 294–306. [CrossRef]
11. Sharma, P.; Kumar, S. Bioremediation of heavy metals from industrial effluents by endophytes and their metabolic activity: Recent advances. *Bioresour. Technol.* **2021**, *339*, 125589. [CrossRef]
12. Hussein, M.; Yoneda, K.; Mohd-Zaki, Z.; Amir, A.; Othman, N. Heavy metals in leachate, impacted soils and natural soils of different landfills in Malaysia: An alarming threat. *Chemosphere* **2021**, *267*, 128874. [CrossRef] [PubMed]
13. Cairns, S.; Todd, A.; Robertson, I.; Byrne, P.; Dunlop, T. Treatment of mine water for the fast removal of zinc and lead by wood ash amended biochar. *Environ. Sci. Adv.* **2022**, *1*, 506–516. [CrossRef]
14. Wierzba, S. Biosorption of lead(II), zinc(II) and nickel(II) from industrial wastewater by Stenotrophomonas maltophilia and Bacillus subtilis. *Pol. J. Chem. Technol.* **2015**, *17*, 79–87. [CrossRef]
15. Budai, P.; Clement, A. Refinement of national-scale heavy metal load estimations in road runoff based on field measurements. *Transp. Res. D Transp. Environ.* **2011**, *16*, 244–250. [CrossRef]
16. Cairns, S.; Robertson, I.; Sigmund, G.; Street-Perrott, A. The removal of lead, copper, zinc and cadmium from aqueous solution by biochar and amended biochars. *Environ. Sci. Pollut. Res.* **2020**, *27*, 21702–21715. [CrossRef]
17. Herath, A.; Datta, D.K.; Bonyadinejad, G.; Salehi, M. Partitioning of heavy metals in sediments and microplastics from stormwater runoff. *Chemosphere* **2023**, *332*, 138844. [CrossRef]
18. Li, W.; Lo, H.-S.; Wong, H.-M.; Zhou, M.; Wong, C.-Y.; Tam, N.F.-Y.; Cheung, S.-G. Heavy metals contamination of sedimentary microplastics in Hong Kong. *Mar. Pollut. Bull.* **2020**, *153*, 110977. [CrossRef]
19. Imhof, H.K.; Laforsch, C.; Wiesheu, A.C.; Schmid, J.; Anger, P.M.; Niessner, R.; Ivleva, N.P. Pigments and plastic in limnetic ecosystems: A qualitative and quantitative study on microparticles of different size classes. *Water Res.* **2016**, *98*, 64–74. [CrossRef] [PubMed]
20. Ta, A.T.; Babel, S. Microplastic contamination on the lower Chao Phraya: Abundance, characteristic and interaction with heavy metals. *Chemosphere* **2020**, *257*, 127234. [CrossRef] [PubMed]
21. Sun, J.; Xia, S.; Ning, Y.; Pan, X.; Qu, J.; Xu, Y. Effects of microplastics and attached heavy metals on growth, immunity, and heavy metal accumulation in the yellow seahorse, Hippocampus kuda Bleeker. *Mar. Pollut. Bull.* **2019**, *149*, 110510. [CrossRef]
22. Khalid, N.; Aqeel, M.; Noman, A.; Khan, S.M.; Akhter, N. Interactions and effects of microplastics with heavy metals in aquatic and terrestrial environments. *Environ. Pollut.* **2021**, *290*, 118104. [CrossRef]
23. Ding, R.; Tong, L.; Zhang, W. Microplastics in Freshwater Environments: Sources, Fates and Toxicity. *Water Air Soil Pollut.* **2021**, *232*, 181. [CrossRef]
24. Qi, K.; Lu, N.; Zhang, S.; Wang, W.; Wang, Z.; Guan, J. Uptake of Pb(II) onto microplastic-associated biofilms in freshwater: Adsorption and combined toxicity in comparison to natural solid substrates. *J. Hazard. Mater.* **2021**, *411*, 125115. [CrossRef]
25. Zhu, S.; Mo, Y.; Luo, W.; Xiao, Z.; Jin, C.; Qiu, R. Aqueous aggregation and deposition kinetics of fresh and carboxyl-modified nanoplastics in the presence of divalent heavy metals. *Water Res.* **2022**, *222*, 118877. [CrossRef] [PubMed]
26. Fu, Q.; Tan, X.; Ye, S.; Ma, L.; Gu, Y.; Zhang, P.; Chen, Q.; Yang, Y.; Tang, Y. Mechanism analysis of heavy metal lead captured by natural-aged microplastics. *Chemosphere* **2021**, *270*, 128624. [CrossRef] [PubMed]
27. European Biochar Foundation. *Guidelines for a Sustainable Production of Biochar*; European Biochar Foundation: Arbaz, Switzerland, 2016; pp. 1–22.

28. Cairns, S.; Robertson, I.; Holliman, P.; Street-Perrott, A. Treatments of wood ash amended biochar to reduce nutrient leaching and immobilise lead, copper, zinc and cadmium in aqueous solution: Column experiments. *Environ. Sci.* **2022**, *8*, 1277–1286. [CrossRef]
29. Cairns, S.; Sigmund, G.; Robertson, I.; Haine, R. Engineered biochar as adsorbent for the removal of contaminants from aqueous medium. In *Engineered Biochar: Fundamentals, Preparation, Characterization and Applications*; Ramola, S., Masek, O., Mendez, A., Tsubota, T., Eds.; Springer Nature: Berlin/Heidelberg, Germany, 2022.
30. Shi, Q.; Guo, S.; Tang, J.; Lyu, H.; Ri, C.; Sun, H. Enhanced removal of aged and differently functionalized polystyrene nanoplastics using ball-milled magnetic pinewood biochars. *Environ. Pollut.* **2023**, *316*, 120696. [CrossRef]
31. Magid, A.S.I.; Islam, S.; Chen, Y.; Weng, L.; Li, J.; Ma, J.; Li, Y. Enhanced adsorption of polystyrene nanoplastics (PSNPs) onto oxidized corncob biochar with high pyrolysis temperature. *Sci. Total Environ.* **2021**, *784*, 147115. [CrossRef]
32. Meng, Z.; Wu, J.; Huang, S.; Xin, L.; Zhao, Q. Competitive adsorption behaviors and mechanisms of Cd, Ni, and Cu by biochar when coexisting with microplastics under single, binary, and ternary systems. *Sci. Total Environ.* **2024**, *913*, 169524. [CrossRef]
33. Li, W.; Meng, J.; Zhang, Y.; Haider, G.; Ge, T.; Zhang, H.; Li, Z.; Yu, Y.; Shan, S. Co-pyrolysis of sewage sludge and metal-free/metal-loaded polyvinyl chloride (PVC) microplastics improved biochar properties and reduced environmental risk of heavy metals. *Environ. Pollut.* **2022**, *302*, 119092. [CrossRef]
34. Cairns, S.; Chaudhuri, S.; Sigmund, G.; Robertson, I.; Hawkins, N.; Dunlop, T.; Hofmann, T. Wood ash amended biochar for the removal of lead, copper, zinc and cadmium from aqueous solution. *Environ. Technol. Innov.* **2021**, *24*, 101961. [CrossRef]
35. Hsieh, L.; He, L.; Zhang, M.; Lv, W.; Yang, K.; Tong, M. Addition of biochar as thin preamble layer into sand filtration columns could improve the microplastics removal from water. *Water Res.* **2022**, *221*, 118783. [CrossRef]
36. Siipola, V.; Pflugmacher, S.; Romar, H.; Wendling, L.; Koukkari, P. Low-cost biochar adsorbents for water purification including microplastics removal. *Appl. Sci.* **2020**, *10*, 788. [CrossRef]
37. Wang, Z.; Sedighi, M.; Lea-Langton, A. Filtration of microplastic spheres by biochar: Removal efficiency and immobilisation mechanisms. *Water Res.* **2020**, *184*, 116165. [CrossRef]
38. Wang, J.; Sun, C.; Huang, Q.X.; Chi, Y.; Yan, J.H. Adsorption and thermal degradation of microplastics from aqueous solutions by Mg/Zn modified magnetic biochars. *J. Hazard. Mater.* **2021**, *419*, 126486. [CrossRef]
39. Tong, M.; He, L.; Rong, H.; Li, M.; Kim, H. Transport behaviors of plastic particles in saturated quartz sand without and with biochar/Fe_3O_4-biochar amendment. *Water Res.* **2020**, *169*, 115284. [CrossRef]
40. Mohan, D.; Kumar, H.; Sarswat, A.; Alexandre-Franco, M.; Pittman, C.U. Cadmium and lead remediation using magnetic oak wood and oak bark fast pyrolysis bio-chars. *Chem. Eng. J.* **2014**, *236*, 513–528. [CrossRef]
41. Shang, J.; Pi, J.; Zong, M.; Wang, Y.; Li, W.; Liao, Q. Chromium removal using magnetic biochar derived from herb-residue. *J. Taiwan Inst. Chem. Eng.* **2016**, *68*, 289–294. [CrossRef]
42. Cairns, S.; Todd, A.M.L.; Robertson, I.; Byrne, P. Metals Removal from Acid Mine Water by Wood-Ash Amended Biochar. In Proceedings of the IMWA, The IMWA 2022, Christchurch, New Zealand, 6–10 November 2022. Available online: https://www.researchgate.net/publication/366325622 (accessed on 22 January 2025).
43. Pagnanelli, F.; Moscardini, E.; Giuliano, V.; Toro, L. Sequential extraction of heavy metals in river sediments of an abandoned pyrite mining area: Pollution detection and affinity series. *Environ. Pollut.* **2004**, *132*, 189–201. [CrossRef]
44. Ahmed, G.; Miah, M.A.; Anawar, H.M.; Chowdhury, D.A.; Ahmad, J.U. Influence of multi-industrial activities on trace metal contamination: An approach towards surface water body in the vicinity of Dhaka Export Processing Zone (DEPZ). *Environ. Monit. Assess.* **2012**, *184*, 4181–4190. [CrossRef]
45. Lokhande, R.S.; Singare, P.U.; Pimple, D.S. Toxicity Study of Heavy Metals Pollutants in Waste Water Effluent Samples Collected from Taloja Industrial Estate of Mumbai, India. 2011. Available online: http://journal.sapub.org/re (accessed on 25 January 2025).
46. Martínez, J.; Hidalgo, M.; Rey, J.; Garrido, J.; Kohfahl, C.; Benavente, J.; Rojas, D. A multidisciplinary characterization of a tailings pond in the Linares-La Carolina mining district, Spain. *J. Geochem. Explor.* **2016**, *162*, 62–71. [CrossRef]
47. Wang, Q.; Wang, B.; Lee, X.; Lehmann, J.; Gao, B. Sorption and desorption of Pb(II) to biochar as affected by oxidation and pH. *Sci. Total Environ.* **2018**, *634*, 188–194. [CrossRef]
48. OECD. *Test No. 106: Adsorption—Desorption Using a Batch Equilibrium Method*; OECD Guidelines for the Testing of Chemicals; OECD: Paris, France, 2000; Section 1. [CrossRef]
49. Gavlová, A.; Jachimowicz, P.; Praus, P.; Bednár, P. Environment changes everything. How relevant are laboratory studies of sorption of pollutants on microplastics? A critical review. *J. Environ. Chem. Eng.* **2025**, *13*, 115655. [CrossRef]
50. Imhoff, P.T.; Akbar Nakhli, S.A. Reducing Stormwater Runoff and Pollutant Loading with Biochar Addition to Highway Greenways. October 2017, pp. 1–47. Available online: https://trid.trb.org/view/1491582 (accessed on 25 January 2025).
51. Kabir, A.H.M.E.; Sekine, M.; Imai, T.; Yamamoto, K.; Kanno, A.; Higuchi, T. Assessing small-scale freshwater microplastics pollution, land-use, source-to-sink conduits, and pollution risks: Perspectives from Japanese rivers polluted with microplastics. *Sci. Total Environ.* **2021**, *768*, 144655. [CrossRef]

52. Lasee, S.; Mauricio, J.; Thompson, W.A.; Karnjanapiboonwong, A.; Kasumba, J.; Subbiah, S.; Morse, A.N.; Anderson, T.A. Microplastics in a freshwater environment receiving treated wastewater effluent. *Integr. Environ. Assess. Manag.* **2017**, *13*, 528–532. [CrossRef]
53. Xue, W.; Maung, G.Y.T.; Otiti, J.; Tabucanon, A.S. Land use-based characterization and source apportionment of microplastics in urban storm runoffs in a tropical region. *Environ. Pollut.* **2023**, *329*, 121698. [CrossRef]
54. Parker-Jurd, F.N.F.; Abbott, G.D.; Guthery, B.; Parker-Jurd, G.M.C.; Thompson, R.C. Features of the highway road network that generate or retain tyre wear particles. *Environ. Sci. Pollut. Res.* **2024**, *31*, 26675–26685. [CrossRef]
55. Parkhurst, D.L.; Appelo, C.A.J. *User's Guide to PHREEQC (Version 2): A Computer Program for Speciation, Batch-Reaction, One-Dimensional Transport, and Inverse Geochemical Calculations*; U.S. Geological Survey Professional Paper; U.S. Geological Survey: Reston, VA, USA, 1999; Volume 312. [CrossRef]
56. McCarroll, D. *Simple Statistical Tests for Geography*; CRC Press: Boca Raton, FL, USA, 2017.
57. Xue, C.; Zhu, L.; Lei, S.; Liu, M.; Hong, C.; Che, L.; Wang, J.; Qiu, Y. Lead competition alters the zinc adsorption mechanism on animal-derived biochar. *Sci. Total Environ.* **2020**, *713*, 136395. [CrossRef]
58. Chirenje, T.; Ma, L.Q.; Lu, L. Retention of Cd, Cu, Pb and Zn by wood ash, lime and fume dust. *Water Air Soil Pollut.* **2006**, *171*, 301–314. [CrossRef]
59. Park, J.H.; Ok, Y.S.; Kim, S.-H.; Cho, J.-S.; Heo, J.-S.; Delaune, R.D.; Seo, D.-C. Competitive adsorption of heavy metals onto sesame straw biochar in aqueous solutions. *Chemosphere* **2016**, *142*, 77–83. [CrossRef]
60. McBride, M.B. *Environmental Chemistry of Soils*; Oxford University Press: New York, NY, USA, 1994.
61. Singh, N.; Khandelwal, N.; Ganie, Z.A.; Tiwari, E.; Darbha, G.K. Eco-friendly magnetic biochar: An effective trap for nanoplastics of varying surface functionality and size in the aqueous environment. *Chem. Eng. J.* **2021**, *418*, 129405. [CrossRef]
62. Trakal, L.; Veselská, V.; Šafařík, I.; Vítková, M.; Číhalová, S.; Komárek, M. Lead and cadmium sorption mechanisms on magnetically modified biochars. *Bioresour. Technol.* **2016**, *203*, 318–324. [CrossRef]
63. Li, X.; Wang, C.; Zhang, J.; Liu, J.; Liu, B.; Chen, G. Preparation and application of magnetic biochar in water treatment: A critical review. *Sci. Total Environ.* **2020**, *711*, 134847. [CrossRef]
64. Zhu, N.; Yan, Q.; He, Y.; Wang, X.; Wei, Z.; Liang, D.; Yue, H.; Yun, Y.; Li, G.; Sang, N. Insights into the removal of polystyrene nanoplastics using the contaminated corncob-derived mesoporous biochar from mining area. *J. Hazard. Mater.* **2022**, *433*, 128756. [CrossRef]
65. Wang, X.; Dan, Y.; Diao, Y.; Liu, F.; Wang, H.; Sang, W.; Zhang, Y. Transport characteristics of polystyrene microplastics in saturated porous media with biochar/Fe_3O_4-biochar under various chemical conditions. *Sci. Total Environ.* **2022**, *847*, 157576. [CrossRef]
66. Mohan, D.; Pittman, C.U.; Bricka, M.; Smith, F.; Yancey, B. Sorption of arsenic, cadmium, and lead by chars produced from fast pyrolysis of wood and bark during bio-oil production. *J. Colloid Interface Sci.* **2007**, *310*, 57–73. [CrossRef]
67. Kemp, W. *Qualitative Organic Analysis Spectrochemical Techniques*, 2nd ed.; McGraw-Hill Book Company: London, UK, 1986.
68. Lima, I.M.; Ro, K.S.; Reddy, G.B.; Boykin, D.L.; Klasson, K.T. Efficacy of Chicken Litter and Wood Biochars and Their Activated Counterparts in Heavy Metal Clean up from Wastewater. *Agriculture* **2015**, *5*, 806–825. [CrossRef]
69. Ali, I.; Tan, X.; Li, J.; Peng, C.; Wan, P.; Naz, I.; Duan, Z.; Ruan, Y. Innovations in the Development of Promising Adsorbents for the Remediation of Microplastics and Nanoplastics—A Critical Review. *Water Res.* **2023**, *230*, 119526. [CrossRef]
70. Zhang, T.; Zhu, X.; Shi, L.; Li, J.; Li, S.; Lü, J.; Li, Y. Efficient removal of lead from solution by celery-derived biochars rich in alkaline minerals. *Bioresour. Technol.* **2017**, *235*, 185–192. [CrossRef]
71. Shi, Y.; Du, J.; Zhao, T.; Feng, B.; Bian, H.; Shan, S.; Meng, J.; Christie, P.; Wong, M.H.; Zhang, J. Removal of nanoplastics from aqueous solution by aggregation using reusable magnetic biochar modified with cetyltrimethylammonium bromide. *Environ. Pollut.* **2023**, *318*, 120897. [CrossRef]
72. Wu, J.; Yang, C.; Zhao, H.; Shi, J.; Liu, Z.; Li, C.; Song, F. Efficient removal of microplastics from aqueous solution by a novel magnetic biochar: Performance, mechanism, and reusability. *Environ. Sci. Pollut. Res.* **2023**, *30*, 26914–26928. [CrossRef] [PubMed]
73. Uchimiya, M.; Lima, I.M.; Klasson, T.; Chang, S.; Wrtelle, L.H.; Rodgers, J.E. Immobilization of Heavy Metal Ions (Cu II, Cd II, Ni II, and Pb II) by Broiler Litter-Derived Biochars in Water and Soil. *J. Agric. Food Chem.* **2010**, *58*, 5538–5544. [CrossRef] [PubMed]
74. Lehmann, J.; Joseph, S. *Biochar for Environmental Management Science, Technology and Implementation*, 2nd ed.; Routledge: Abingdon, UK, 2015.
75. Ganie, Z.A.; Khandelwal, N.; Tiwari, E.; Singh, N.; Darbha, G.K. Biochar-facilitated remediation of nanoplastic contaminated water: Effect of pyrolysis temperature induced surface modifications. *J. Hazard. Mater.* **2021**, *417*, 126096. [CrossRef] [PubMed]